The Stable Diiron(2.5) Complex Ion $[(NC)_5Fe(\mu\text{-tz})Fe(CN)_5]^{5-}$, tz = 1,2,4,5-Tetrazine, and Its Neighboring Oxidation States

Markus Glöckle,† Wolfgang Kaim,*,† Axel Klein,† Emil Roduner,‡ Georg Hübner,‡ Stanislav Zalis,§ Joris van Slageren,‖ Franz Renz,⊥ and Philipp Gütlich⊥

Institut für Anorganische Chemie, Universität Stuttgart, Pfaffenwaldring 55, D-70550 Stuttgart, Germany, Institut für Physikalische Chemie, Universität Stuttgart, Pfaffenwaldring 55, D-70550 Stuttgart, Germany, J. Heyrovsky Institute of Physical Chemistry, Academy of Sciences of the Czech Republic, Dolejškova 3, CZ-18223 Prague, Czech Republic, Anorganisch Chemisch Laboratorium, Institute of Molecular Chemistry, Universiteit van Amsterdam, Nieuwe Achtergracht 166, NL-1018 WV Amsterdam, The Netherlands, and Institut für Anorganische Chemie, Johannes-Gutenberg-Universität, Saarstrasse 21, D-55122 Mainz, Germany

Received November 6, 2000

The conceptually simple mixed-valent diiron compound $(NEt_4)_5[(NC)_5Fe(\mu\text{-tz})Fe(CN)_5]$ with the 1,2,4,5-tetrazine (tz) bridging ligand was obtained as a thermally and air-stable material that displays large and highly variable electrochemical comproportionation constants between about 10^8 (in water) and $10^{19.0}$ (in acetonitrile). Strong metal−metal interaction is also evident from spectroscopic results obtained for the solid and for the dissolved species. The rather intense intervalence charge-transfer band occurs around 2400 nm; infrared and Mössbauer spectra reveal the high spectroscopic symmetry of the system according to an $(Fe^{2.5})_2$ formulation. DFT calculations on the $[(NC)_5Fe(\mu\text{-tz})Fe(CN)_5]^{6-}$ ion confirm the presence of very low-lying π^*(tz) and high-lying d(Fe) orbitals.

Introduction

Mixed-valence compounds[1] with two or more metal centers in similar or identical settings have become interesting because of their role in biochemistry ($Fe_n^{II,III}$, $Mn_n^{II,III,IV}$, $Cu_2^{I,II}$),[2] their model character for intramolecular electron-transfer reactivity,[3] their special spectroscopic or other physical properties,[1,4] their potential in "molecular electronics",[5] and their function as test systems for theoretical approaches.[6]

Following the discovery of the conceptually simple yet chemically stable mixed-valent complex ion $[(H_3N)_5Ru(\mu\text{-pz})Ru(NH_3)_5]^{5+}$ (pz = pyrazine), the Creutz−Taube ion,[7] a large number of related molecule-bridged diruthenium(II,III) systems have been investigated.[8] The Creutz−Taube ion is distinguished by a relatively high comproportionation constant $K_c \approx 10^7$ according to eq 1 in various solvents[7−9] and by an intense,

$$K_c = e^{nF\Delta E/(RT)} = \frac{[M^{(n-1)}]^2}{[M^n][M^{(n-2)}]}$$

$$M^n + M^{(n-2)} \rightleftarrows 2M^{(n-1)} \qquad (1)$$

asymmetric intervalence charge-transfer (IVCT) band at 1570 nm in the near-infrared; it is now considered to be a delocalized system with metal center equivalence even on the time scale ($\sim 10^{-13}$ s) of vibrational spectroscopy.

Although $Fe_n^{II,III}$ systems are common in the geo- and biosphere,[1,2] small nonorganometallic[10] diiron(II,III) species corresponding to the Creutz−Taube ion have remained rare because of the lability, e.g. of the ammine−iron bond (high-spin situation). The stability of the prototypical mixed-valent coordination compound $Fe^{III}_4[Fe^{II}(CN)_6]_3$ (Prussian Blue, Blue Iron Pigment[11]) has thus prompted searches for other mixed-valent iron cyanide species; however, simple bis(cyanoiron) complexes with low-spin configurations were reported to exhibit only weak metal−metal interaction with poorly established mixed-valent intermediate states.[12,13] For instance, the $[(NC)_5Fe(\mu\text{-pz})Fe(CN)_5]^{5-}$ ion was reported to have $K_c = 10^{1.7}$ in aqueous solution.[12] Recent studies of $[(NC)_5Fe(\mu\text{-pz})Fe(CN)_5]^{5-}$ in aprotic polar media showed, however, that this species could be stabilized to $K_c = 10^{6.5}$ (in CH_3CN),[14] in agreement with

* To whom correspondence should be addressed: Telephone: +49 711 685-4170. Fax: +49 711 685-4165. E-mail: kaim@iac.uni-stuttgart.de.
† Institut für Anorganische Chemie, Universität Stuttgart.
‡ Institut für Physikalische Chemie, Universität Stuttgart.
§ Heyrovsky Institute of Physical Chemistry.
‖ Universiteit van Amsterdam.
⊥ Johannes-Gutenberg-Universität.

(1) (a) Robin, M. B.; Day, P. *Adv. Inorg. Chem. Radiochem*. **1967**, *10*, 247. (b) Prassides, K., Ed. *Mixed Valency Systems*−*Applications in Chemistry, Physics and Biology*; Kluwer Academic Publishers: Dordrecht, The Netherlands, 1991.
(2) Kaim, W.; Bruns, W.; Poppe, J.; Kasack, V. *J. Mol. Struct.* **1993**, *292*, 221.
(3) Taube, H. *Angew. Chem.* **1984**, *96*, 315; *Angew. Chem., Int. Ed. Engl.* **1984**, *23*, 329.
(4) McCleverty, J. A.; Ward, M. D. *Acc. Chem. Res.* **1998**, *31*, 842.
(5) Ward, M. D. *Chem. Soc. Rev.* **1995**, *34*, 121.
(6) (a) Hush, N. S. *Prog. Inorg. Chem.* **1967**, *8*, 391. (b) Sutin, N. *Prog. Inorg. Chem.* **1983**, *30*, 441. (c) Hush, N. S. *Coord. Chem. Rev.* **1985**, *64*, 135. (d) Bencini, A.; Ciofini, I.; Daul, C. A.; Ferretti, A. *J. Am. Chem. Soc.* **1999**, *121*, 11418.
(7) Creutz, C.; Taube, H. *J. Am. Chem. Soc.* **1973**, *95*, 1086.
(8) Creutz, C. *Prog. Inorg. Chem.* **1983**, *30*, 1.
(9) Creutz, C.; Chou, M. H. *Inorg. Chem.* **1987**, *26*, 2995.
(10) For examples of ferrocene/ferrocenium mixed-valent systems: Kurosawa, M.; Nankawa, T.; Matsuda, T.; Kubo, K.; Kurihara, M.; Nishihara, H. *Inorg. Chem.* **1999**, *38*, 5113.
(11) (a) Herren, F.; Fischer, P.; Ludi, A.; Hälg, W. *Inorg. Chem.* **1980**, *19*, 956. (b) Ludi, A. *Chem. Unserer Zeit* **1988**, *22*, 123. (c) Buxbaum, G., Ed. *Industrial Inorganic Pigments*, 2nd ed.; Wiley-VCH: Weinheim, 1998; p 131.
(12) Felix, F.; Ludi, A. *Inorg. Chem.* **1978**, *17*, 1782.
(13) Hennig, H.; Rehorek, A.; Rehorek, D.; Thomas, P. *Inorg. Chim. Acta* **1984**, *86*, 41.

10.1021/ic001229i CCC: $20.00
Published on Web 04/06/2001

the extremely strong response of cyanoiron compounds to solvent effects.[15] Since the lability of partially delocalized[14] $[(NC)_5Fe(\mu\text{-pz})Fe(CN)_5]^{5-}$ precluded more detailed investigation, we chose neutral 1,2,4,5-tetrazine (tz) derivatives with their extremely low-lying π^* orbitals as bridging ligands for bis(cyanoiron) species.[16,17] Mixed-valent compounds related to the Creutz–Taube ion use the π^* MO of the conjugated bridge for effecting metal–metal interaction (electron-transfer coupling pathway).[18]

In the following we describe the results obtained for the most simple of such systems, the tz-bridged bis(pentacyanoiron) complex ion $[(NC)_5Fe(\mu\text{-tz})Fe(CN)_5]^{5-}$ ($\mathbf{1}^{5-}$) and the corresponding redox system $\mathbf{1}^{n-}$ (n = 7, 6, 5,4; tetraethylammonium counterions).[17] In contrast to other isolable molecule-bridged diiron(II,III) complexes,[19–21] the $\mathbf{1}^{5-}$ ion exhibits surprising electrochemical and chemical stability *without* extra support from multiple bridging or chelate ligands. Results are reported from solid-state and solution studies, and DFT calculations on the $\mathbf{1}^{6-}$ ion were used to illustrate the underlying molecular orbital situation.

Although it is an excellent π acceptor and potentially tetradentate ligand, unsubstituted 1,2,4,5-tetrazine (tz) has rarely been used in coordination chemistry. Some dinuclear carbonylmetal(0) species were reported and a diosmium(II) system exists;[22] however, all attempts to obtain a bis(pentaammineruthenium) compound failed presumably because of proton-coupled electron-transfer reactions of the extremely reducible tz heterocycle. In contrast, the bis(pentacyanoiron) compound described in the following is even isolable in two oxidation states, a homovalent diiron(II) and an unusually stable mixed-valent form.

Results and Discussion

Synthesis. The diiron(II) precursor compound $(NEt_4)_6(\mathbf{1}^{6-})$ was obtained as a dihydrate from tz and in situ prepared $(NEt_4)_3[Fe(NH_3)(CN)_5]$[17] in H_2O. The dark-green complex is stable in water but dissociates above −25 °C in CH_3CN or CH_2Cl_2. ^1H NMR and Mössbauer results (cf. below) confirm the low-spin iron(II) configuration. The dark-blue mixed-valent $(NEt_4)_5(\mathbf{1}^{5-})\cdot 2H_2O$ was isolated[17] after oxidation of the precursor with *p*-(*N*,*N*-dimethylamino)benzenediazonium hexafluorophosphate;[23] it is stable in air as a solid and in solution, in water, *and* in aprotic solvents. Two further neighboring oxidation states could be studied after chemical oxidation of $\mathbf{1}^{5-}$ ($\rightarrow\mathbf{1}^{4-}$) or electrochemical reduction of $\mathbf{1}^{6-}$ ($\rightarrow\mathbf{1}^{7-}$). The mononuclear $(NEt_4)_3[(tz)Fe(CN)_5]$ was also prepared for comparison.[17] The results from the spectroscopic, electrochemical, and spectroelectrochemical characterization are summarized in Tables 1–5, and Figures 1–9 illustrate salient features.

Table 1. Electrochemical Data[a] of Compounds

compound	$E_{1/2(Ox1)}$	$E_{1/2(Ox2)}$	$E_{1/2(Red1)}$	K_c	solvent[b]
tz[c]			−1.16		CH_3CN
$\{(tz)[Fe(CN)_5]\}^{3-}$	−0.32		−1.73		CH_3CN
$\{(tz)[Fe(CN)_5]\}^{3-}$	−0.23		nd		CH_2Cl_2 [d]
$\{(tz)[Fe(CN)_5]\}^{3-}$	−0.38		−1.85[e]		DMF[f]
$\{(tz)[Fe(CN)_5]\}^{3-}$	0.36[g]		−0.82[e,g]		H_2O[h]
$\{(\mu\text{-tz})[Fe(CN)_5]_2\}^{6-}$ [i]	−0.93	−0.03	−1.91	$10^{19.0}$	CH_3CN
$\{(\mu\text{-tz})[Fe(CN)_5]_2\}^{6-}$ [i]	−0.85	0.00	−1.65[n]	$10^{17.8}$	CH_2Cl_2 [d]
$\{(\mu\text{-tz})[Fe(CN)_5]_2\}^{6-}$ [i]	−0.94	−0.13	−2.32[e]	$10^{17.5}$	DMF[f]
$\{(\mu\text{-tz})[Fe(CN)_5]_2\}^{6-}$ [i]	0.14[g]	0.64[g,j]	nd	$\sim 10^{7.9}$	H_2O[h]
$\{(\mu\text{-pz})[Fe(CN)_5]_2\}^{6-}$ [k]	−0.92	−0.60	nr	$10^{6.5}$	CH_3CN
$\{(\mu\text{-pz})[Ru(NH_3)_5]_2\}^{4+}$ [l]	0.44	0.87	nr	$10^{7.3}$	CH_3CN
$\{(\mu\text{-pz})[Ru(NH_3)_5]_2\}^{4+}$ [m]	0.37[m]	0.76[m]	nr	$10^{6.6}$	H_2O

[a] Half-wave potentials $E_{1/2}$ in V vs the ferrocene/ferrocenium couple, unless stated otherwise. Cyclic voltammetry at 200 mV/s. [b] 0.1 M Bu_4NPF_6 and 298 K, unless stated otherwise. [c] From ref 25. [d] 0.2 M Bu_4NPF_6, 240 K. [e] Cathodic peak potential for irreversible process. [f] 233 K, 1% CH_3OH added for better solubility. [g] Potentials vs $[Fe(CN)_6]^{3-/4-}$. [h] 0.25 M Na_2SO_4. [i] Identical results were obtained with the 5− ion. [j] Anodic peak potential (electrode adsorption). [k] From ref 14. [l] From ref 9. [m] From ref 8, values against NHE. [n] Anodic peak potential.

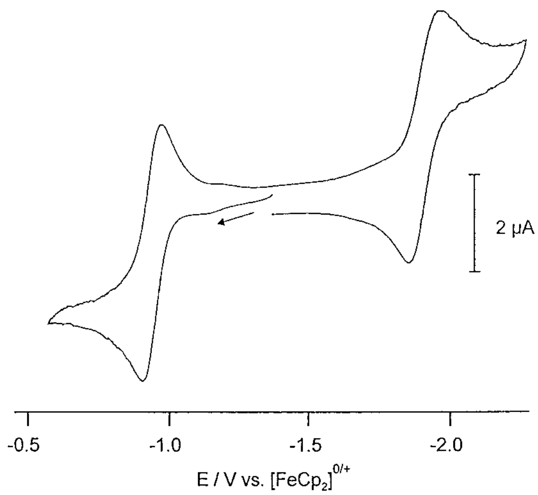

Figure 1. Cyclic voltammogram of $(NEt_4)_6(\mathbf{1})$ in CH_3CN/0.1 M NBu_4PF_6 at 238 K (50 mV/s scan rate).

Cyclic Voltammetry. System $\mathbf{1}^{n-}$, n = 4–7, exhibits three separated and electrochemically reversible one-electron waves in acetonitrile at low temperatures (Table 1 and Figure 1).[17] The potentials are slightly shifted in other aprotic solvents (Table 1) where some processes may be less reversible; water is an extreme case with an irreversible oxidation $\mathbf{1}^{5-/4-}$. In any case, there is obviously an enormous increase in K_c on going from the pz- to the tz-bridged system, i.e., from $10^{1.9}$ to about $10^{8.0}$ in water and from $10^{6.5}$ to $10^{19.0}$ in acetonitrile. The absolute values for K_c as well as the very strong solvent dependence of K_c are extraordinary (Table 1); other low-spin $Fe^{II}Fe^{III}$ complexes bridged by an organic ligand were reported with $K_c = 10^{8.5}$.[20] The possibility of hydrogen bonding from water to the free nitrogen atoms of the tetrazine and/or to the cyanide ligands appears to strongly attenuate the capability of the π acceptor bridging ligand to mediate metal–metal interaction.

Despite a metal–metal distance of about 6.8 Å,[24] the very low-lying π^* MOs of tz effect a strong stabilization of the

(14) Ketterle, M.; Kaim, W.; Olabe, J. A.; Parise, A. R.; Fiedler, J. *Inorg. Chim. Acta* **1999**, *291*, 66.
(15) (a) Toma, H. E.; Takasugi, M. S. *J. Solution Chem.* **1983**, *12*, 547. (b) Toma, H. E.; Takasugi, M. S. *J. Solution Chem.* **1989**, *18*, 576.
(16) (a) Ketterle, M.; Fiedler, J.; Kaim, W. *J. Chem. Soc., Chem. Commun.* **1998**, 1701. (b) Glöckle, M.; Fiedler, J.; Katz, N. E.; Garcia Posse, M.; Cutin, E.; Kaim, W. *Inorg. Chem.* **1999**, *38*, 3270.
(17) Glöckle, M.; Kaim, W. *Angew. Chem.* **1999**, *111*, 3262; *Angew. Chem., Int. Ed.* **1999**, *38*, 3072.
(18) (a) Kaim, W.; Kasack, V. *Inorg. Chem.* **1990**, *29*, 4696. (b) Haga, M.; Matsumura-Inoue, T.; Yamabe, S. *Inorg. Chem.* **1987**, *26*, 4148.
(19) (a) Hartman, J. A. R.; Rardin, R. L.; Chaudhuri, P.; Pohl, K.; Wieghardt, K.; Nuber, B.; Weiss, J.; Papaefthymiou, G. C.; Frankel, R. B.; Lippard, S. J. *J. Am. Chem. Soc.* **1987**, *109*, 7387. (b) Albela, B.; Bill, E.; Brosch, O.; Weyhermüller, T.; Wieghardt, K. *Eur. J. Inorg. Chem.* **2000**, 139.
(20) (a) Mountford, H. S.; MacQueen, D. B.; Li, A.; Otvos, J. W.; Calvin, M.; Krankel, R. B.; Spreer, L. O. *Inorg. Chem.* **1994**, *33*, 1748. (b) Spreer, L. O.; Li, A.; MacQueen, D. B.; Allan, C. B.; Otwos, J. W.; Calvin, M.; Frankel, R. B.; Papaefthymiou, G. C. *Inorg. Chem.* **1994**, *33*, 1753.
(21) Lee, D.; Krebs, C.; Huynh, B. H.; Hendrich, M. P.; Lippard, S. J. *J. Am. Chem. Soc.* **2000**, *122*, 5000.
(22) (a) Herberhold, M.; Süss-Fink, M. *Z. Naturforsch.* **1976**, *31b*, 1489. (b) Glöckle, M.; Kaim, W. Unpublished results.
(23) Connelly, N. G.; Geiger, W. E. *Chem. Rev.* **1996**, *96*, 877.

Table 2. Absorption Data[a] of Complexes

complex	λ_{max} (ϵ) $\Delta\tilde{\nu}_{1/2}$[a]	solvent[b]
$\{(tz)[Fe(CN)_5]\}^{3-}$	263 (sh), 299 (sh), 690 (7.18) **4930**	CH_3CN
$\{(tz)[Fe(CN)_5]\}^{3-}$	297 (sh), 706	CH_2Cl_2
$\{(tz)[Fe(CN)_5]\}^{3-}$	438, 705	CH_3OH
$\{(tz)[Fe(CN)_5]\}^{3-}$	214 (10.39), 245 (sh), 423 (1.05), 685 (7.83) **4000**	H_2O
$\{(\mu\text{-tz}^{\bullet -})[Fe^{II}(CN)_5]_2\}^{7-}$ [c]	375 (1.86), 676 (3.72)	CH_3CN (240 K)
$\{(\mu\text{-tz})[Fe^{II}(CN)_5]_2\}^{6-}$	284 (sh), 353,[d] 520 (1.62), 543 (sh), 1021 (21.67) **2620**	CH_3CN (233 K)
$\{(\mu\text{-tz})[Fe^{II}(CN)_5]_2\}^{6-}$	1014	CH_2Cl_2 (233 K)
$\{(\mu\text{-tz})[Fe^{II}(CN)_5]_2\}^{6-}$	234, 272 (sh), 372, 486, 919	CH_3OH
$\{(\mu\text{-tz})[Fe^{II}(CN)_5]_2\}^{6-}$	219 (18.85), 258 (sh), 395 (sh), 452 (1.33), 848 (22.00) **2990**	H_2O
$\{(\mu\text{-tz})[Fe^{2.5}(CN)_5]_2\}^{5-}$	304 (4.44), 345 (3.71), 678 (13.07) *4190*, 2520[e] (1.15) **860**	CH_3CN
$\{(\mu\text{-tz})[Fe^{2.5}(CN)_5]_2\}^{5-}$	267 (sh), 295 (3.46), 321 (3.22), 402 (1.42), 439 (sh), 744 (15.06) **3740**, 2250[e] (2.82) **970**	D_2O
$\{(\mu\text{-tz})[Fe^{III}(CN)_5]_2\}^{4-}$	414 (2.02), 630 (6.19) **4140**	CH_3CN (238 K)
$\{(\mu\text{-pz})[Fe^{II}(CN)_5]_2\}^{6-}$ [f]	406 (3.40), 599 (17.40)	CH_3CN
$\{(\mu\text{-pz})[Fe(CN)_5]_2\}^{5-}$ [f]	406 (4.40), 599 (7.30), 745 (8.00), 2475 (3.90) **1500**	CH_3CN
$\{(\mu\text{-pz})[Fe^{III}(CN)_5]_2\}^{4-}$ [f]	406 (5.80)	CH_3CN
$\{(\mu\text{-pz})[Ru(NH_3)_5]_2\}^{5+}$ [g]	1600	CH_3CN
$\{(\mu\text{-pz})[Ru(NH_3)_5]_2\}^{5+}$ [h]	1570 (5.00) **1400**	H_2O

[a] Wavelengths λ of absorption maxima in nm, molar extinction coefficients (ϵ) in 10^{-3} M^{-1} cm^{-1}, bandwidth at half-height $\Delta\tilde{\nu}_{1/2}$ in cm^{-1}. [b] Measurements at 298 K unless stated otherwise. [c] From spectroelectrochemistry. [d] Low intensity. [e] From ref 17. [f] From ref 14. [g] From ref 9. [h] From ref 8.

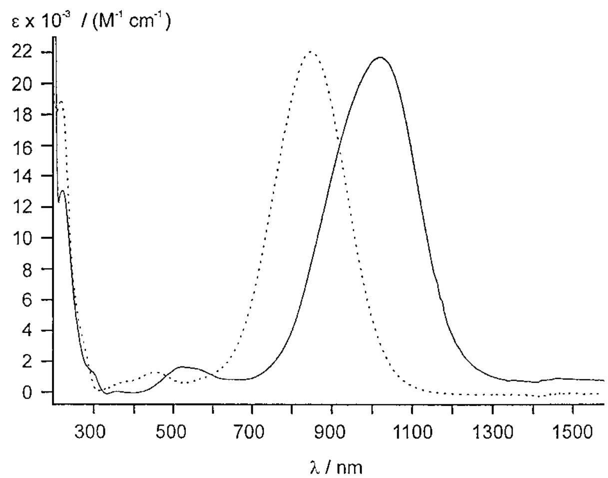

Figure 2. Absorption spectra of $(NEt_4)_6(\mathbf{1})$ in CH_3CN at 233 K (—) and in H_2O at 298 K (···).

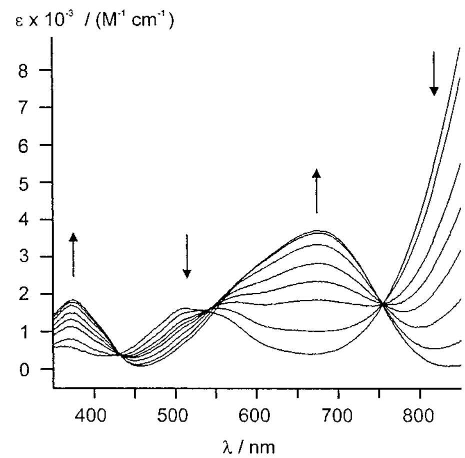

Figure 3. Spectroelectrochemical reduction of $(NEt_4)_6(\mathbf{1})$ to the radical anion in CH_3CN/0.1 M NBu_4PF_6 at 240 K.

d^5/d^6 mixed-valent intermediate; the additional factor of 10^5 in comparison to bis(tetracyanoiron) complexes of bis(chelating) tetrazine ligands[16] is attributed to the less negative charge and the restricted orientation of the cyanometal moieties in these latter systems.

The reduction potentials of the mononuclear and especially of the dinuclear complex are cathodically shifted with respect to that of the free ligand[25] (Table 1). This result reflects the high negative charges and strong dπ* back-bonding in these species and stands in contrast to what is observed with neutral complex fragments bridged by a reducible π acceptor ligand.[26]

Absorption Spectroscopy. Both the $\mathbf{1}^{6-}$ and $\mathbf{1}^{5-}$ complex ions exhibit intense, solvatochromic[15,27] metal-to-ligand charge transfer (MLCT) absorptions at rather long wavelengths, between 680 and 1050 nm (Table 2 and Figure 2). This unusually low transition energy illustrates the stabilization of the tetrazine π* MO, qualitatively confirmed by DFT calculations (cf. below); corresponding features lie at about 600 nm for the pyrazine-bridged analogue.[14] The mononuclear complex $(NEt_4)_3[(tz)Fe(CN)_5]$ and the $\mathbf{1}^{7-}$ form (generated by low-temperature spectroelectrochemistry; Figure 3) show similar bands at somewhat higher energies (Table 2). The in situ generated diiron(III) complex $\mathbf{1}^{4-}$ also absorbs strongly in the visible; the band at 630 nm (15870 cm^{-1}) is tentatively assigned to an LMCT transition involving the cyanide ligands.

The presence of fully reversible electrochemical waves in acetonitrile allows us to compare electrochemical potential differences ΔE (in V) with optical transition energies E_{op} (in eV).[28] For the $\mathbf{1}^{6-}$ form the values $\Delta E = 0.98$ V and $E_{op} =$ 1.21 eV indicate a relatively small reorganization energy parameter $\xi = E_{op} - \Delta E = 0.23$ (e)V, which is slightly larger than the values established for polypyridylruthenium species.[28b] The onset of the MLCT band at about 1270 nm (Figure 2) corresponds to 7870 cm^{-1}, or 0.98 eV, and thus coincides with ΔE.

The intervalence charge-transfer (IVCT) feature expected[1,8] for the mixed-valent state $\mathbf{1}^{5-}$ occurs in the near-infrared at 2520

(24) Schwach, M.; Hausen, H.-D.; Kaim, W. *Inorg. Chem.* **1999**, *38*, 2242.
(25) Fischer, H.; Müller, T.; Umminger, I.; Neugebauer, F. A. *J. Chem. Soc., Perkin Trans. 2* **1988**, 413.
(26) Gross, R.; Kaim, W. *Inorg. Chem.* **1986**, *25*, 498.
(27) Reichardt, C. *Solvents and Solvent Effects in Organic Chemistry*, 2nd ed.; VCH: Weinheim, 1988.
(28) (a) Kober, E. M.; Goldsby, K. A.; Narayana, D. N. S.; Meyer, T. J. *J. Am. Chem. Soc.* **1983**, *105*, 4303. (b) Dodsworth, E. S.; Lever, A. B. P. *Chem. Phys. Lett.* **1985**, *119*, 61; **1986**, *124*, 152. (c) Kaim, W.; Klein, A. *Organometallics* **1995**, *14*, 1176.

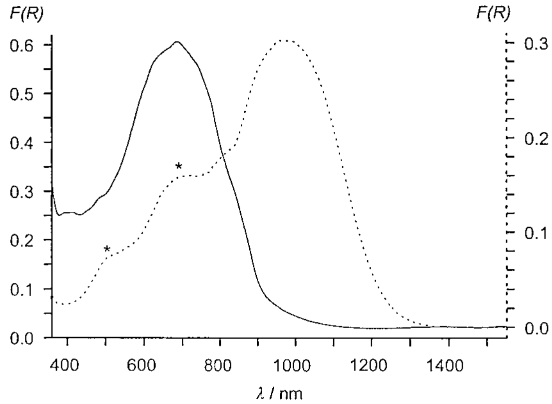

Figure 4. Vis−NIR reflectance spectra, transformed to $F(R)$, of $(NEt_4)_6(\mathbf{1})$: $2H_2O$ (···) and $(NEt_4)_5(\mathbf{1})\cdot 2H_2O$ (−) (∗ indicates artifact peaks).

nm (3970 cm^{-1}) in acetonitrile and at 2250 nm (4440 cm^{-1}) in aqueous solution (D_2O) as an asymmetrical band.[17] The IVCT band intensity is more than twice as large in D_2O (Table 2), while the bandwidth at half-height remains virtually unchanged at about 900 cm^{-1}. The latter number lies well below the ca. 3200 cm^{-1} calculated from the Hush formula,[6,8]

$$\Delta\tilde{\nu}_{1/2} = (2310\ cm^{-1}\ \tilde{\nu}_{max})^{1/2} \qquad (2)$$

for weakly coupled centers, indicating a class III[1a] mixed-valent system for $\mathbf{1}^{5-}$, as already suggested by the huge K_c values. The electronic interaction constant V_{AB} may thus be estimated[6,8] at $\nu_{IVCT}/2 = 2220\ cm^{-1}$ (D_2O) or 1980 cm^{-1} (CH_3CN).

In ammineruthenium mixed-valence chemistry the solvent dependence of the IVCT band has been often used as a criterion for assignment to either class II (localized valences, solvent sensitivity) or class III (delocalized valences, no solvent effect).[1a,8] Compound $(NEt_4)_5[(NC)_5Fe(\mu\text{-tz})Fe(CN)_5]$ exhibits a slight negative solvatochromism, i.e., increasing IVCT band energy with increasing "polarity" as quantified by Gutmann's acceptor number (AN).[27,29] The effect, ranging from ν(IVCT) = 3970 cm^{-1} for CH_3CN (AN 18.9) via ν(IVCT) = 4250 cm^{-1} for CD_3OD (AN 41.3) to ν(IVCT) = 4440 cm^{-1} for D_2O (AN 54.8 for H_2O), is rather small, however, and may be traced to hydrogen bonding rather than general solvation. We thus do not conclude from this small solvent effect that $\mathbf{1}^{5-}$ should be a class II mixed-valent species.

For absorption data independent of solvent influence we measured the diffuse reflectance spectra of $(NEt_4)_6[(NC)_5Fe(\mu\text{-tz})Fe(CN)_5]\cdot 2H_2O$ and $(NEt_4)_5[(NC)_5Fe(\mu\text{-tz})Fe(CN)_5]\cdot 2H_2O$. The transformed spectra (Figure 4) yield MLCT absorption features similar to those found in solvents (Table 2). The intervalence band for $(NEt_4)_5[(NC)_5Fe(\mu\text{-tz})Fe(CN)_5]\cdot 2H_2O$ was also observed by reflectance spectroscopy (Figure 5). The wavelength λ = 2495 nm (4010 cm^{-1}) at the absorption maximum is rather similar to the values found for dissolved species (Table 2), and the bandwidth $\Delta\nu_{1/2} = 1450\ cm^{-1}$ remains again well below the 3040 cm^{-1} calculated from the Hush formula (eq 2) for weakly coupled systems.[6] We thus conclude that the process of dissolution does not significantly alter the iron−iron interaction; the class III classification remains unchanged.

Vibrational Spectroscopy. Infrared spectroscopy of system $\mathbf{1}^{n-}$ reveals a reduced number of discernible cyanide stretching features because of typical band overlap,[12,14,30] both in solution (IR spectroelectrochemistry) and in the solid (reflectance spectrum). The high-energy shift of the band from $\mathbf{1}^{6-}$ via $\mathbf{1}^{5-}$ to $\mathbf{1}^{4-}$ (optically transparent thin-layer electrode (OTTLE) spectroelectrochemistry[31]) is as expected for the oxidation going through a valence-delocalized intermediate.[32] There is a small (10 cm^{-1}) splitting discernible for the mixed-valent system that, however, does not signify valence localization;[32] it occurs similarly for the mononuclear iron(II) complex $(NEt_4)_3[(tz)Fe(CN)_5]$ (Table 3 and Figure 6).

Most significantly, there is no specific aromatic ring vibration band visible in the IR spectrum between 1500 and 1700 cm^{-1} for the mixed-valent state. Such bands were found for pyrazine-bridged analogues;[14,33,34] they indicate loss of spectroscopic

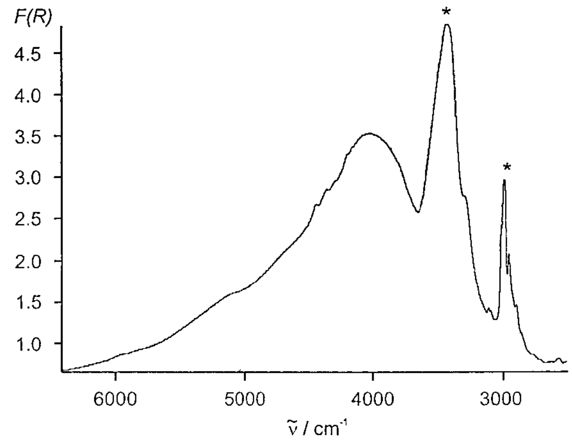

Figure 5. IR reflectance spectrum, transformed to $F(R)$, of $(NEt_4)_5(\mathbf{1})\cdot 2H_2O$ (∗ indicates OH and CH vibration peaks).

Table 3. Cyanide Stretching Vibrations[a] of Complexes

complex	$\tilde{\nu}_{CN}$[a]
$\{(tz)[Fe^{II}(CN)_5]\}^{3-}$	2106 (sh), 2097 m, 2082 s
$\{(\mu\text{-tz}^{\bullet-})[Fe^{II}(CN)_5]_2\}^{7-}$ [b]	2043 (sh), 2032 s
$\{(\mu\text{-tz})[Fe^{II}(CN)_5]_2\}^{6-}$ [c]	2087 (sh), 2067 vs
$\{(\mu\text{-tz})[Fe^{2.5}(CN)_5]_2\}^{5-}$	2110 s, 2101 s
$\{(\mu\text{-tz})[Fe^{III}(CN)_5]_2\}^{4-}$ [b]	2123 (sh), 2117 w
$\{(\mu\text{-pz})[Fe^{II}(CN)_5]_2\}^{6-}$ [d]	2044 s
$\{(\mu\text{-pz})[Fe(CN)_5]_2\}^{5-}$ [d]	2112 w, 2070 (br)
$\{(\mu\text{-pz})[Fe^{III}(CN)_5]_2\}^{4-}$ [d]	2112 w

[a] Wavenumbers of absorption maxima in cm^{-1}. Measurements in acetonitrile at 298 K, unless noted otherwise. [b] From spectroelectrochemistry at 240 K. [c] At 240 K. [d] From ref 14.

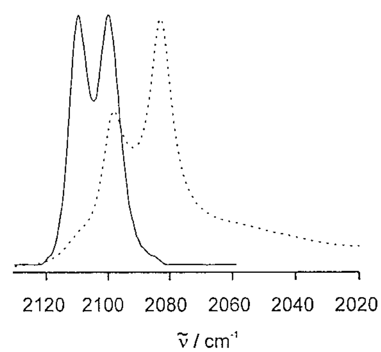

Figure 6. IR absorption spectra of $(NEt_4)_5(\mathbf{1})$ (−) and $(NEt_4)_3[(tz)Fe(CN)_5]$ (···) in CH_3CN at 298 K.

(29) Gutmann, V.; Resch, G.; Linert, W. *Coord. Chem. Rev.* **1982**, *43*, 133.
(30) Best, S. P.; Clark, R. J. H.; McQueen, R. C. S.; Joss, S. *J. Am. Chem. Soc.* **1989**, *111*, 548.
(31) Krejcik, M.; Danek, M.; Hartl, F. *J. Electroanal. Chem.* **1991**, *317*, 179.
(32) Atwood, C. G.; Geiger, W. E. *J. Am. Chem. Soc.* **2000**, *122*, 5477.

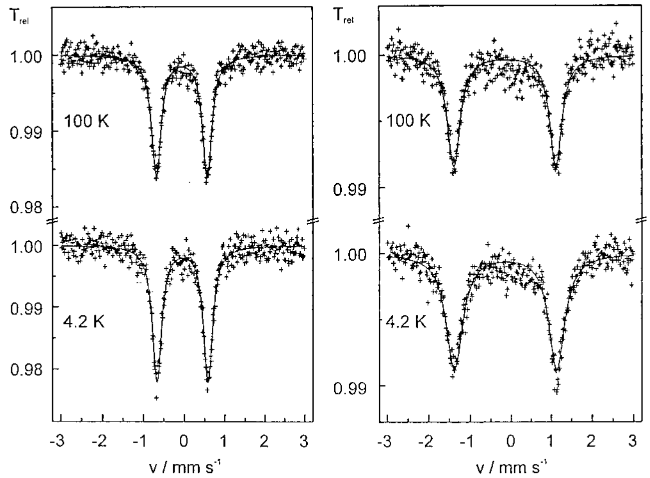

Figure 7. Mössbauer spectra of $(NEt_4)_6(\mathbf{1})\cdot 2H_2O$ (left) and $(NEt_4)_5(\mathbf{1})\cdot 2H_2O$ (right) at 100 and 4.2 K.

Table 4. ^{57}Fe Mössbauer Parameters[a] for $\mathbf{1}^{6-}$ and $\mathbf{1}^{5-}$

	$[(CN)_5Fe^{II}(tz)Fe^{II}(CN)_5]^{6-}$ ($\mathbf{1}^{6-}$)			$[(CN)_5Fe^{2.5}(tz)Fe^{2.5}(CN)_5]^{5-}$ ($\mathbf{1}^{5-}$)		
T (K)	δ (mm s^{-1})	ΔE_Q (mm s^{-1})	Γ (mm s^{-1})	δ (mm s^{-1})	ΔE_Q (mm s^{-1})	Γ (mm s^{-1})
100	0.063(4)	1.245(6)	0.144(6)	−0.021(6)	2.510(6)	0.188(9)
4.2	0.077(4)	1.251(6)	0.139(6)	−0.008(6)	2.514(6)	0.246(9)

[a] δ = isomer shift, ΔE_Q = quadrupole splitting, Γ = line width. Statistical standard deviations are given in parentheses.

inversion symmetry (nonzero dipole moment) and thus at least partial valence localization. In the present case we therefore postulate valence delocalization on the time scale of vibrational spectroscopy, implying an intramolecular electron-transfer rate $k_{ET} > 10^{13}$ s^{-1} and an oxidation state formulation $(Fe^{2.5})_2$.

Mössbauer Spectroscopy. ^{57}Fe Mössbauer spectra of $(NEt_4)_6[(NC)_5Fe(\mu\text{-tz})Fe(CN)_5]\cdot 2H_2O$ and $(NEt_4)_5[(NC)_5Fe(\mu\text{-tz})Fe(CN)_5]\cdot 2H_2O$ were recorded at 100 and 4.2 K (see Figure 7). Least-squares-fitted parameters are listed in Table 4. The Mössbauer spectrum of the diiron(II) compound at 4.2 K shows a doublet that is characteristic of nitroprussiate analogues[35] with their low isomer shift and high lattice contribution to the quadrupole splitting for an Fe^{II} in the low spin state.[36] Although not as low as the $\delta = -0.257$ mm s^{-1} for nitroprussiate itself, the near-zero value of δ for $\mathbf{1}^{6-}$ indicates the superior π acceptor properties of tetrazine ligands. Similar values were reported for hexacyanoferrate(II) and for the pentacyanoferrate(II) complex of *N*-methylpyrazine.[35] The $\mathbf{1}^{6-}$ ion shows less deviation from cubic symmetry than $Na_2[Fe(CN)_5(NO)]$ because its quadrupole splitting is smaller by 0.57 mm s^{-1}. The Mössbauer spectrum at 100 K exhibits the same behavior. The Mössbauer spectra of the mixed-valent compound at 4.2 and 100 K show only one doublet—evidence for valence delocalization on the Mössbauer time scale.[19,20] No reduction of the quadrupole splitting between 4.2 and 100 K is observed. This indicates that the axial splitting of the ^{2}T term into an ^{2}E term and ^{2}A term, with the ^{2}A term being lowest, is so large that the ^{2}E term could not be thermally populated.

(33) Scheiring, T.; Kaim, W.; Olabe, J. A.; Parise, A. R.; Fiedler, J. *Inorg. Chim. Acta* **2000**, *300*−*302*, 125.
(34) Hornung, F.; Baumann, F.; Kaim, W.; Olabe, J. A.; Slep, L. D.; Fiedler, J. *Inorg. Chem.* **1998**, *37*, 311, 5402.
(35) Toma, H. E.; Giesbrecht, E.; Malin, J. M.; Fluck, E. *Inorg. Chim. Acta* **1975**, *14*, 11.
(36) Gütlich, P.; Link, R.; Trautwein, A. *Mössbauer Spectroscopy and Transition Metal Chemistry*; Springer: Berlin, 1978.

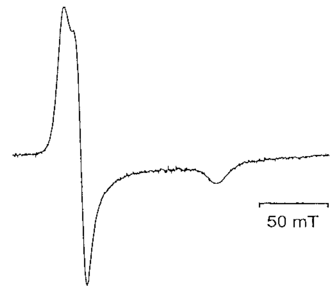

Figure 8. X-band EPR spectrum of $(NEt_4)_5(\mathbf{1})$ in glassy frozen CH_3CN at 3.7 K.

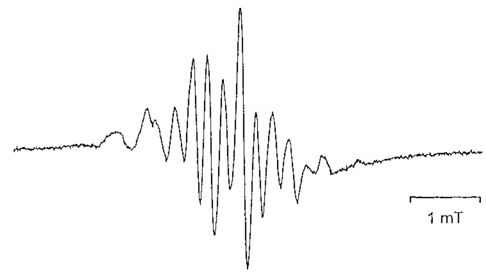

Figure 9. X-band EPR spectrum of electrochemically generated $\mathbf{1}^{7-}$ in CH_3CN/0.1 M NBu_4PF_6 at 235 K.

Table 5. EPR Data[a] of Paramagnetic Compounds

compound	g_1	g_2	g_3	$\langle g\rangle^b$	solvent	temp (K)
$\{(\mu\text{-tz})[Fe^{2.5}(CN)_5]_2\}^{5-}$	2.531	2.422	1.794	2.27	CH_3CN	3.7
$\{(\mu\text{-pz})[Fe(CN)_5]_2\}^{5-}$	2.45	2.45	1.79	2.25	CH_3CN	3.7
$\{(\mu\text{-pz})[Ru(NH_3)_5]_2\}^{5+}$	2.799	2.489	1.346	2.21	*c*	4
$\{(\mu\text{-tz})[Fe(CN)_5]_2\}^{7-}$				2.0041^d	CH_3CN	235
$\{(\mu\text{-tz})[Mo(CO)_5]_2\}^{-}$				2.0047^e	THF	298

[a] X-band data. [b] Calculated average or measured isotropic *g* values. [c] Single crystal study, from ref 38. [d] Hyperfine coupling $a_N = 0.69$ mT (2N), $a_{N'} = 0.48$ mT (2N). [e] Hyperfine coupling $a_N = 0.705$ mT (2N), $a_{N'} = 0.433$ mT (2N); from ref 40.

Scheme 1

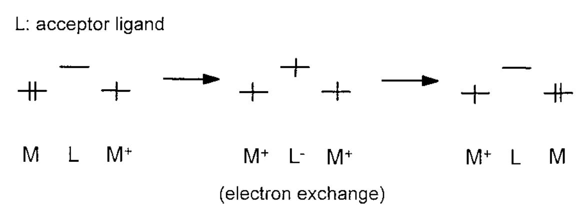

EPR Spectroscopy. The two paramagnetic states $\mathbf{1}^{5-}$ and $\mathbf{1}^{7-}$ reveal very different EPR characteristics (Figures 8 and 9 and Table 5). In agreement with the mixed-valent formulation the former shows iron-centered spin, as is evident from rapid relaxation (observed only at low temperatures), from the calculated $\langle g\rangle = 2.27$ and from the large g anisotropy (Table 5). Similar values of $g_{1,2} \approx 2.5$ and $g_3 \approx 1.7$ have been reported for bis(tetracyanoiron(2.5)) species,[16] other low-spin $Fe^{III}Fe^{II}$ systems,[14,19] and conventional low-spin iron(III) centers (d^5 situation).[37] In the absence of hyperfine information[2] it is thus not immediately conspicuous by EPR that the spin is symmetrically delocalized over two equivalent iron centers. According to Scheme 1,[18a] even a strong participation of the bridging acceptor ligand in mediating the metal−metal interaction does not manifest itself by EPR spectroscopy because of vanishing spin density of the central moiety in a three-center

(37) Walker, F. A. *Coord. Chem. Rev.* **1999**, *185*−*186*, 471.

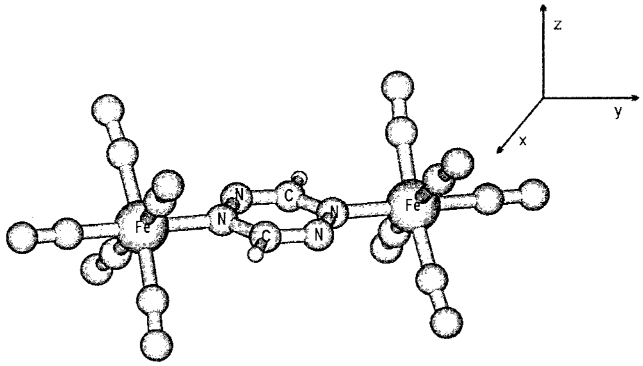

Figure 10. $\{(\mu\text{-tz})[Fe(CN)_5]_2\}^{n-}$ molecule with orientation of axes.

Table 6. Calculated Bond Lengths (Å) and Angles (deg) of $\mathbf{1}^{6-}$ and $\mathbf{1}^{5-}$

	$\mathbf{1}^{6-}$	$\mathbf{1}^{5-}$
Fe−N(CN)$_{cis}$	1.968	1.962
Fe−N(CN)$_{trans}$	1.931	1.928
Fe−N (tz)	2.090	2.073
N1−N2 (tz)	1.372	1.361
N1−C (tz)	1.361	1.358
N2−C (tz)	1.332	1.330
C−N (CN)$_{cis}$	1.185	1.182
C−N (CN)$_{trans}$	1.187	1.181
Fe−N1−N2	124.6	123.5
Fe−N1−C	122.7	122.5
N1−N2−C	118.2	117.7
N1−C−N2	129.1	128.0

orbital approach. The larger g anisotropy measured for the Creutz−Taube ion[38] is most likely due to the higher spin−orbit coupling factor of Ru relative to Fe.

Low-temperature reduction of $\mathbf{1}^{6-}$ to $\mathbf{1}^{7-}$ in very dry acetonitrile gave a resolved EPR spectrum with $g = 2.0041$, clearly indicating a ligand-centered spin.[39] The spectrum and the extracted data are similar to those reported for $[(OC)_5M(\mu\text{-tz})M(CO)_5]^{\bullet-}$, M = Cr, Mo, or W,[40] i.e., dominating ^{14}N quintets from the two coordinated and the two uncoordinated tetrazine nitrogen centers (Figure 9 and Table 5).

DFT Calculation Results. The DFT calculations on $\mathbf{1}^{n-}$, $n = 6, 5$, were performed in C_{2h} constrained symmetry, the z axis coinciding with the C_2 symmetry axis and the tetrazine ligand lying in the xy plane. Two geometrical arrangements were considered: the first with the equatorial cyanide ligands at 45° relative to the symmetry plane and the second with those CN ligands lying in the symmetry plane. The former configuration has a slightly lower energy, and all further results correspond to this optimized geometry. The optimized ADF/BP geometry of $\mathbf{1}^{6-}$ is depicted in Figure 10, and calculated bond lengths and angles are listed in Table 6.

The ADF/BP calculated one-electron scheme of $\mathbf{1}^{6-}$ is depicted in Figure 11, indicating the composition of the molecular orbitals. The set of the highest molecular orbitals is formed by the almost degenerate $25a_g$, $25b_u$, $24a_g$, and $24b_u$ MOs, composed mainly of the $d_{x^2-y^2}$ and d_{xy} non-π orbitals of the two iron centers. The lower lying $15b_g$ and $14a_u$ molecular orbitals are formed by the $Fe^{II}(CN)_5$ fragment π orbitals (d_{yz}) mixing with the tz π^* orbitals. The tz π^* orbital contributes to $15b_g$ and $14a_u$ with 3% and 28%, respectively. The LUMO, $15a_u$, is mainly composed from the π^* orbital (a_u) of the tz ligand (70%) with contributing d_{yz} orbitals of the iron centers.

(38) Stebler, A.; Ammeter, J. H.; Fürholz, U.; Ludi, A. *Inorg. Chem.* **1984**, *23*, 2764.
(39) Kaim, W. *Coord. Chem. Rev.* **1987**, *76*, 187.

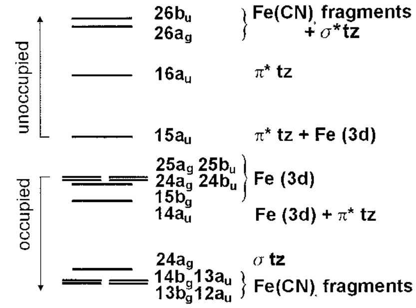

Figure 11. Molecular orbital scheme of $\mathbf{1}^{6-}$.

Table 7. TD DFT Calculated Lowest Singlet Excitation Energies and Oscillator Strengths for $\mathbf{1}^{6-}$

state	main component (%)	transition energy in eV (nm)	oscillator strength
^1B_g	99 ($25b_u \rightarrow 15a_u$)	0.85 (1441)	<0.001
^1A_u	99 ($25a_g \rightarrow 15a_u$)	0.85 (1441)	<0.001
^1B_g	99 ($24b_u \rightarrow 15a_u$)	0.94 (1319)	<0.001
^1A_u	99 ($24a_g \rightarrow 15a_u$)	0.95 (1305)	<0.001
^1B_u	91 ($15b_g \rightarrow 15a_u$)	1.61 (770)	0.330
^1B_u	92 ($15b_g \rightarrow 16a_u$)	2.17 (571)	0.117
^1B_u	99 ($14b_g \rightarrow 15a_u$)	2.74 (452)	0.016

During reduction the added electron is accepted in MO $15a_u$, which confirms the interpretation of EPR data for $\mathbf{1}^{7-}$. For the mixed-valent species $\mathbf{1}^{5-}$, the lowest energy corresponds to the configuration ^2B_g where the unpaired electron is located in the π $15b_g$ molecular orbital. Calculated bond lengths and angles for the ^2B_g configuration of $\mathbf{1}^{5-}$ are listed in Table 6. According to a recent calculation approach to the Creutz−Taube ion by Bencini et al.,[6d] the potential energy surface (PES) was calculated in the direction of the antisymmetric Fe−N(tz) stretching mode, looking for energy minima corresponding to possible symmetry breaking. The calculation started from the C_{2h} optimized geometry of $\mathbf{1}^{5-}$. During the PES calculation the Fe−Fe distance was kept constant at 6.944 Å, Fe−N(tz) varied from the equilibrium position ($r(\text{Fe−N}) = r(\text{Fe−N})_{opt} + \Delta r$ and $r(\text{Fe−N}') = r(\text{Fe−N})_{opt} - \Delta r$), and the rest of the molecule was optimized. No additional minima were found on the PES for C_s symmetry, which indicates the delocalized ground state of $\mathbf{1}^{5-}$.

Table 7 lists the lower singlet excitation energies calculated for $\mathbf{1}^{6-}$. The lowest excited states ^1B_g and ^1A_u correspond to excitations from the $25a_g$, $25b_u$, $25a_g$, and $24b_u$ molecular orbitals into the LUMO $15a_u$. These overlap-disfavored transitions have very low oscillator strengths. The most intense transition $15b_g \rightarrow 15a_u$ (MLCT) is calculated at 1.61 eV (770 nm), i.e., at higher energy than the experimentally observed band (848 nm in H_2O, 1021 nm in CH_3CN; Table 2).

From these first calculation results we can conclude that the huge comproportionation constants for the mixed-valent $\mathbf{1}^{5-}$ ion result from the close-lying and well overlapping dπ(Fe) and π^*(tz) orbitals. Within the electron-transfer alternative for molecule-mediated metal−metal communication,[18] the enormous π back-donation from the Fe^{II} center to the bridge strongly increases the donor strength of the tz ligand, which in turn stabilizes the Fe^{III} center at the other end. Conversely, the electron-withdrawing effect of Fe^{III} further enhances the already considerable π acceptor capability of tz with respect to electron-rich Fe^{II}; both solvent-dependent effects work synergistically to stabilize the mixed-valent state as quantified by large K_c values.

The DFT calculation results on the closed-shell $\mathbf{1}^{6-}$ ion are also in agreement with rather low-energy IVCT (d → d) transitions within the near-degenerate set of non-π d(Fe) orbitals. The $\mathbf{1}^{5-}$ ion is clearly valence-delocalized and does not follow the Hush approximation (eq 2) for weakly coupled systems. On the other hand, the long wavelength of the IVCT transition reflects only moderately strong electronic coupling between the iron(2.5) centers. More detailed calculations on the mixed-valent form, its excited states, and the effects of the environment will be attempted.

Experimental Section

General Methods. All operations were carried out under an argon atmosphere. EPR spectra were recorded in the X band on a Bruker ESP 300E system equipped with a Bruker ER035M gaussmeter and a HP 5350B microwave counter. Infrared spectra were obtained using a Perkin-Elmer Paragon 1000 PC instrument. Diffuse reflectance IR spectra were obtained with a Nicolet Magna 560 FTIR spectrometer and Praying Mantis equipment. UV/vis/NIR absorption spectra were recorded on a Bruins Instruments Omega 10 spectrophotometer. Diffuse reflectance UV/vis/NIR spectra were recorded and transformed (Kubelka−Munk function[41]) using the Bruins Instruments Omega program package (version 5.40). Cyclic voltammetry was carried out using a three-electrode configuration (glassy carbon or Pt working electrode, Pt counter electrode, Ag/AgCl reference) and a PAR 273 potentiostat and function generator. The ferrocene/ferrocenium couple served as the internal reference. Spectroelectrochemical measurements were performed using an optically transparent thin-layer electrode (OTTLE) cell[31] for UV/vis and IR spectra and a two-electrode capillary for EPR studies.[42] ^{57}Fe Mössbauer spectra of compounds $\mathbf{1}^{n-}$, $n = 6, 5$, have been recorded using a conventional spectrometer mounted in a helium cryostat with temperature variation between 4 and 300 K. The isomer shift values in Table 4 are relative to α-iron. For the source, ^{57}Co in rhodium was used. The data were evaluated with the program MOSFUN.[43]

Synthetic procedures for preparation of the species described have been reported.[17]

DFT Calculations. Ground-state electronic structure calculations on the complexes $\mathbf{1}^{n-}$, $n = 6, 5$, have been done on the basis of the density-functional theory (DFT) method using the ADF1999[44,45] program package. DFT calculations on $\mathbf{1}^{5-}$ were spin-unrestricted. The lowest excited states of the closed-shell complex were calculated by time-dependent DFT (TD DFT).[46]

Within the ADF program, Slater type orbital basis sets of triple-ζ (Fe) and double-ζ (H, C, and N) quality with polarization functions were employed. The inner shells were represented by the frozen core approximation (1s for C, N and 1s−2s for Fe were kept frozen). The following density functionals were used in ADF: the local density approximation (LDA) with VWN parametrization of electron gas data and the functional including Becke's gradient correction[47] to the local exchange expression in conjunction with Perdew's gradient correction[48] to the LDA expression (ADF/BP).

Acknowledgment. This work has been supported by the Deutsche Forschungsgemeinschaft, the Volkswagenstiftung, and the Fonds der Chemischen Industrie. S. Zalis thanks the Ministry of Education of the Czech Republic (Grant OC.D14.20) for financial support.

IC001229I

(40) Kaim, W.; Kohlmann, S. *Inorg. Chem.* **1986**, *25*, 3442.
(41) Kubelka, P.; Munk, F. *Z. Tech. Phys.* **1931**, *12*, 593.
(42) Kaim, W.; Ernst, S.; Kasack, V. *J. Am. Chem. Soc.* **1990**, *112*, 173.
(43) Müller, E. W. Program MOSFUN. Ph.D. Thesis, Johannes-Gutenberg-Universität, Mainz, Germany, 1980.
(44) Baerends, E. J.; Bérces, A.; Bo, C.; Boerrigter, P. M.; Cavallo, L.; Deng, L.; Dickson, R. M.; Ellis, D. E.; Fan, L.; Fischer, T. H.; Fonseca Guerra, C.; van Gisbergen, S. J. A. Groeneveld, J. A.; Gritsenko, O. V.; Harris, F. E.; van den Hoek, P.; Jacobsen, H.; van Kessel, G.; Kootstra, F.; van Lenthe, E.; Osinga, V. P.; Philipsen, P. H. T.; Post, D.; Pye, C. C.; Ravenek, W.; Ros, P.; Schipper, P. R. T.; Schreckenbach, G.; Snijders, J. G.; Sola, M.; Swerhone, D.; te Velde, G.; Vernooijs, P.; Versluis, L.; Visser, O.; van Wezenbeek, E.; Wiesenekker, G.; Wolff, S. K.; Woo, T. K.; Ziegler, T. ADF 1999.01; Vrije Universiteit: Amsterdam, 1999.
(45) Fonseca Guerra, C.; Snijders, J. G.; te Velde, G.; Baerends, E. J. *Theor. Chem. Acc.* **1998**, *99*, 391.
(46) van Gisbergen, S. J. A.; Snijders, J. G.; Baerends, E. J. *Comput. Phys. Commun.* **1999**, *118*, 119.
(47) Becke, A. D. *Phys. Rev. A* **1988**, *38*, 3098.
(48) Perdew, J. P. *Phys. Rev. A* **1986**, *33*, 8822.